AN IMAGE ASSOCIATION MODEL OF THE BRODMANN AREAS

Douglas S. Greer
General Manifolds

Abstract

The ability to associate images is the basis for learning relationships involving vision, hearing, tactile sensation, and kinetic motion. A new architecture is described that has only local, recurrent connections, but can directly form global image associations. This architecture has many similarities to the structure of the neocortex, including the division into Brodmann areas, the distinct internal and external lamina, and the pattern of neuron interconnection.

Analogous to the bits in an SR flip-flop, two arbitrary images can hold each other in place in an association processor and thereby form a short-term image memory. Overlay masks can focus attention on specific image regions. Spherically symmetric wavelets, identical to those found in the receptive fields of the retina, enable efficient image computations. Stability and noise reduction in reciprocal continuous wavelet transform representations can be achieved using an orthogonal projection based on the reproducing kernel.

keywords: *Natural intelligence; cognitive signal processing; memory; pattern recognition; mathematical models.*

1. INTRODUCTION

Throughout its entire extent, the cerebral cortex is composed of the same six cellular layers. Based on the relative thickness of these layers, the cerebral cortex of humans is divided into approximately fifty Brodmann areas [1], [2]. Between Brodmann areas, these layers vary in thickness, but within each area, they are roughly the same.

A cross section of the neocortex first published by Brodmann and Vogt almost one hundred years ago is shown as the background illustration in Fig. 1. The six cellular layers are labeled I through VI. Layers II and IV are the *external and internal granule* layers respectively, while layers III and V are the *external and internal pyramidal* layers. In addition, on the right side of Fig. 1, which has been prepared with a Weigert stain, the *external and internal Bands of Baillarger*, labeled 4 and 5b are visible. A complete theory of natural intelligence must somehow account for this uniform structure, and the existence of the two nearly identical (external and internal) parallel systems.

Also shown in the center of Fig. 1 is a loop representing a cortical column created from the local connections between neurons in the various layers. Even though most neurons have a width of only a few microns, they form layers of constant thickness over the full extent of the Brodmann areas, which may be several square centimeters in size. These facts are consistent with an image association model.

We use the term *image* or *field* in a general mathematical sense for a scalar or vector valued function defined on a manifold [3], [4], for example an open region of the plane ($\mathbb{R}^2$). We use script letters to denote function transforms, for example the wavelet transform of a function f is written as $\mathcal{W}[f]$.

Each layer of each Brodmann area can be considered to be one image. Consequently, the general notion of an image plays a role in cognition that extends beyond computer vision. For example, we can model an audio spectrogram that represents time in the horizontal dimension and frequency in the vertical dimension as a two-dimensional image. Similar tonotopic maps exist at several locations in the central nervous system (CNS) [1], [5].

The generalization of images to include any function defined on a manifold is a powerful one in terms of its ability to describe and model many natural phenomena. Images can include mass (external world), position (location of the body surface), energy (visible light and sound vibrations), and force (pressure on the body surface and the tension on the combined muscle cross-sections).

For example, the surface of the skin (a somatotopic map) can be modeled as a two-dimensional manifold and its position in space then becomes a vector valued function defined on that space. A manifest of the two-

dimensional images that are processed by the CNS is extensive [6], and includes retinotopic maps, spatial maps, and kinetic maps.

In this context, learning and retrieving image associations can be viewed as a basic cognitive function. As an example, when a child learns a new word, say "horse", they learn an association between two images: the visual image of a picture of a horse and the two-dimensional audio spectrogram of the sound of the word "horse".

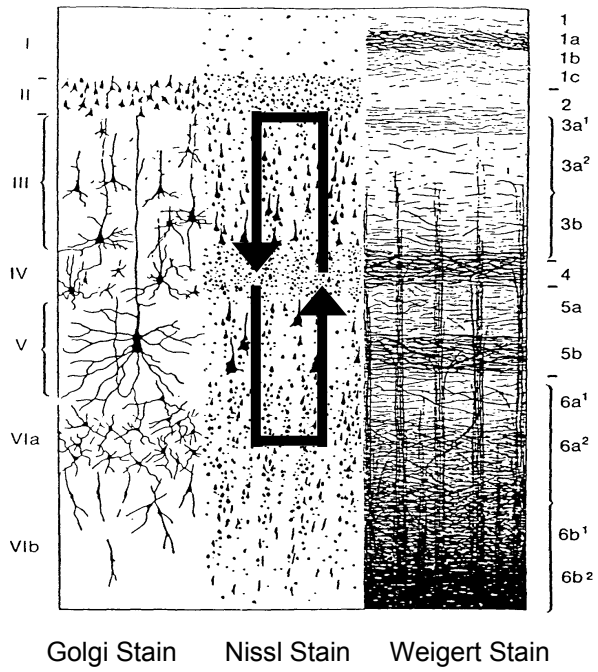

Fig. 1. A cross-section of the cortex showing the six cortical layers. Most of the structures occur in external/internal pairs such as the granual layers (II and IV), the pyramidal layers (III and V) and the Bands of Baillarger (4 and 5b). The loop in the center depicts the connections of a single cortical column. (background from Brodmann & Vogt, 1908).

We discuss three types of Manifold Association Processors (MAPs). The first two MAP types are abstract and are intentionally defined only in terms of their external, observable behavior. The first of these, the Λ-MAP model is stateless, but can perform logic operations by producing the output image that is associated with multiple input images. The SR-MAP is constructed from two Λ-MAPs and is analogous to a set-reset flip-flop where the individual bits have been replaced by two-dimensional images. The Ψ-MAP description specifies the internal principles of operation. Its unique design uses a recurrent neural network to integrate the results of many locally connected processing elements into an overall global image association.

Borrowing from the terminology of digital design, specifically a programmable logic array, the term Ψ-MAP *Array* is used to specify an interconnected collection of Ψ-MAPs where the bits are again replaced by images.

Spectral representations, in particular wavelets, encode weighted averages over large regions with their coefficients. Spherically symmetric wavelets, similar to the receptive fields of the retina, allow image associations to be computed faster and more efficiently. We hypothesize that these wavelet-like fields are not unique to the visual system but are a general principle of operation that governs the entire cerebral cortex.

The continuous wavelet transform contains redundant information that is characterized by the reproducing kernel [7]. When associations are formed between image spectral representations, this redundant information can be used to reduce errors and create stability.

1.1. Related Work

A Ψ-MAP array is an implementation of an abstract symbol processing system. Consequently, descriptions of cognitive models that can be expressed in terms of symbolic operations [8], [9] can be used to evaluate Ψ-MAPs, which use images to represent symbols. Control masks, in particular time-varying control masks, act as instructions for directing the operation of the array. Therefore, the ability to recall control mask images translates into the ability to recall procedures that operate on symbols. Cognitive informatics describes how the acquisition, representation, retrieval, and comprehension of concepts may be expressed as an aggregation of symbols and operators [10], [11]. These theoretical frameworks can be applied in the analysis of Ψ-MAP arrays as computational engines that evaluate semantic functions.

In contrast to some previous work that uses feature detection and extraction and performs the analysis in a lower dimensional space, we discuss algorithms where the images maintain their topological structure and the associations take place directly between the image wavelet transforms.

Willshaw [12] first proposed a model of associative memories using non-holographic methods. Bidirectional associative memories were originally proposed by Kosko [13] and subsequently developed by others [14]. These neural networks are designed such that all of the outputs directly depend on all the inputs, that is, they require global connections to the entire input image.

Consequently, implementations can suffer from poor performance for high-resolution images or large training sets. Cellular neural networks, first described by Chua and Yang [15], are implemented with local connections, but do not use spectral methods or aggregate multiple images with a unified control structure.

A second type of neural-network associative memory is created by following the trajectory of a particle in a dynamical system governed by a recurrence of the form $\vec{x}_{i+1} = f(\vec{x}_i)$. The association is not fixed in time but is the relationship between a starting point and a final fixed point of the dynamical system. To distinguish between these two types of association mechanisms we will refer to the second type as a classification, where each unique fixed point identifies a *class* that equals the set of all points whose trajectory leads to that point. The Ψ-MAP model may also go through a classification phase, but once the association is formed, the relationship between the associated images is static and explicit.

Wavelet networks combine the functional decomposition of wavelets with the parameter estimation and learning capacity of neural networks [16]–[18]. However, these differ from the Ψ-MAP methods in their lack of reciprocal fields and the associations formed between spectral representations. Moreover, their use of wavelet basis functions rather than the continuous wavelet transform implies that the projection based on the reproducing kernel will not reduce noise and add stability since the basis functions are by definition linearly independent.

2. ASSOCIATION PROCESSORS

We can consider an arbitrary collection of photographs as a set of symbols. If we wish to represent numbers or letters, we can pick a font and record images of their alphanumeric glyph. Similarly, fixed-time snapshots of any two-dimensional computational map can be used as symbols representing external stimuli or motor control actions.

Imagine a black box that takes an image as its input and associates with it an arbitrary output image. This abstract black box represents a two-dimensional manifold association processor. A MAP can also take multiple images as inputs and produce multiple image outputs. The output of a multi-input MAP may depend on all of its inputs. This abstract Λ-MAP (Λ from the Greek word *Logikos*) can perform logic operations but is stateless. It does not remember past values, and its output image depends only on the current values of its input images. In Fig. 2 we show a two-input, single-output Λ-MAP.

If symbols are represented as images then a two-input, single-output Λ-MAP can function as an arithmetic logic unit [19]. Imagine ten photographic images of the digits zero through nine. By learning two hundred binary associations, the Λ-MAP can memorize the addition and multiplication tables. If two images are used to represent "Condition X is True/False", then any Boolean operation can be learned by memorizing four image associations. Thus, a Λ-MAP is logically complete and consequently, with additional memory and control components, it can simulate the operation of any digital computer.

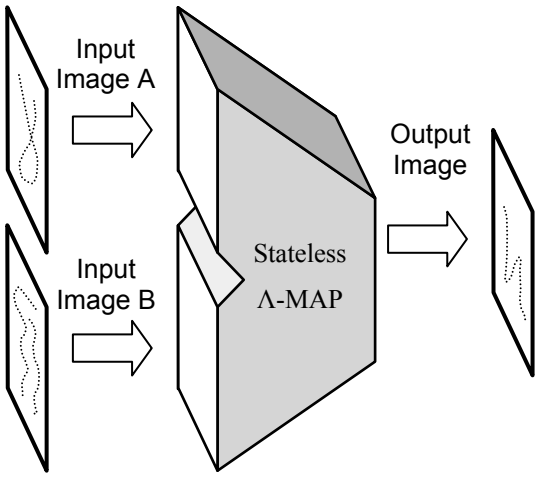

Fig. 2. The abstract Logic Manifold Association Processor or Λ-MAP produces an output image that is associated with its input images. It is stateless in that its current output does not depend on the previous inputs.

Internally, inside each bit of SRAM, is a logic circuit equivalent to the inverter loop shown in Figure 3A. This circuit has two stable states, corresponding to values of *Q* equal to zero or one. In Figure 3B we show the logic diagram of an SR flip-flop which is designed using two NAND gates and is equivalent to an inverter ring when the set (*S'*) and reset (*R'*) control inputs are both one. If the *S'* or *R'* inputs momentarily go to zero the flip-flop will set or reset and remain there until either the *S'* or *R'* input is changed again.

Like addition and multiplication, logic operations are abstract laws of mathematics. Consequently, the recurrence that creates memory from stateless NAND gates is in essence a fundamental law of nature.

Suppose we replace the single bits *S'*, *R'*, *Q* and *Q'* in the SR flip-flop with two-dimensional images and we replace the two NAND gates with two Λ-MAPs. This *Set-Reset Manifold Association Processor* (SR-MAP) is shown in Fig. 4, where the output *Q'* is relabeled as *P*.

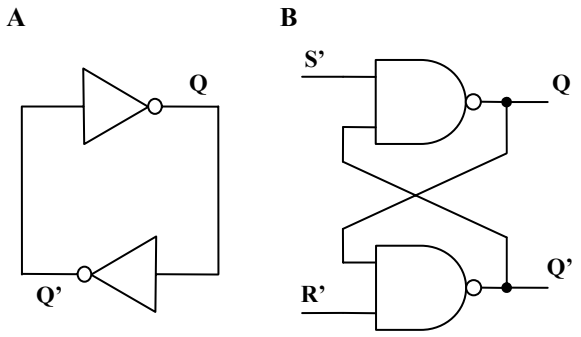

Fig. 3. An example of how memory can be constucted from logic. The fundamental unit of memory, a single bit, can be formed from two logic gates by creating a circuit with a feedback loop. (*A*) Two inverters in a ring "lock in place" a single bit and its complement. (*B*) When the set (S') and reset (R') inputs are both one, an SR flip-flop is logically equivalent to an inverter ring.

Referring to Fig. 4, let $\Lambda_E(S, P) = Q$ denote the external Λ-MAP, and let $\Lambda_I(Q, R) = P$ denote the internal Λ-MAP.

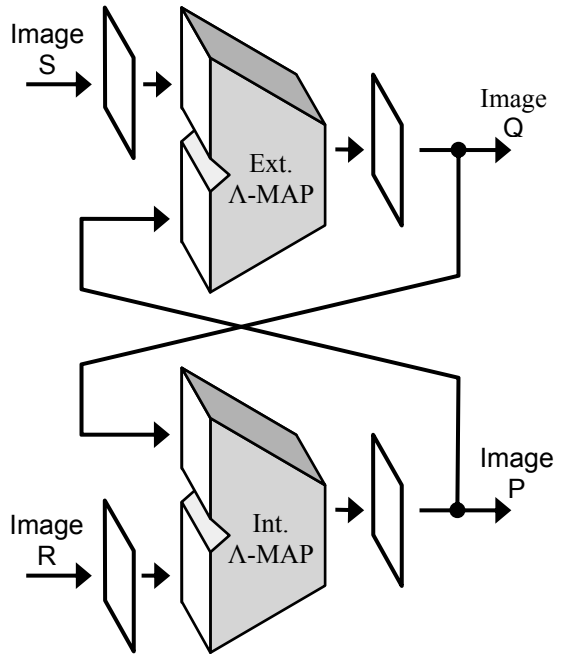

Fig. 4. The Set-Reset Manifold Association Processor or SR-MAP is analogous to the SR flip-flop where the NAND gates have been replaced by Λ-MAPs. The two Λ-MAPs are labeled Ext. and Int. and correspond to the external in internal lamina of the neocortex.

Let *Null* denote a predefined "blank" image, and let $\{(a_1, b_1), (a_2, b_2) \ldots (a_i, b_i) \ldots (a_n, b_n)\}$ be an arbitrary collection of n image pairs. Suppose we program Λ_E such that $\Lambda_E(Null, b_i) = a_i$ for all i, and program Λ_I such that $\Lambda_I(a_i, Null) = b_i$ for all i. When the R and S inputs are Null, the SR-MAP will have n stable states corresponding to the n image pairs (a_i, b_i). We will refer to the images that form an image pair (a_i, b_i) as *reciprocal* images.

In addition to the above, suppose we have n input images $(s_1, s_2, \ldots, s_n)$ and we add the additional associations to Λ_E such that $\Lambda_E(s_i, X) = a_i$ for any image X. Then by changing the S input from Null to s_i, we can force the SR-MAP from whatever state it is currently in to the state identified by the reciprocal image pair (a_i, b_i). If the S input now returns to Null, the SR-MAP will remain in this state, until either the S or R input image changes again.

2.1. Local Support

We would like to construct the MAPs with processing elements similar to neural networks. However, the performance of image association processors begins to degrade for high-resolution images when every pixel in the input image is directly used in the calculation of each output pixel. The same is true when too many input/output pairs are used in the neural network training. Consequently, to construct a MAP with a large number of high resolution associations, a new type of design is required.

We partition the overall neural network and define an abstract local Processing Element (PE). Each PE(i,j) accepts a small set of real-valued inputs and produces a single real-valued output corresponding to the pixel (i,j) in the output image. We will use the term *lattice* to describe a collection of PEs which forms an entire output image. Each PE has $m_{i,j}$ input connections where $m_{i,j}$ is much smaller than the total number of pixels in an input image. Such a network partition is illustrated in Fig. 5.

The particular set of inputs chosen for PE(i,j) could be based on a two-dimensional Density Function (DF) similar to a two-dimensional probability density function [20]. Pixels in the input image where the DF is relatively larger are more likely to be used as inputs to a particular PE.

We define the *support* of a PE to be those points in the image where the DF is non-zero. If the support of a PE is contained in a region of radius d, where d is small relative to the size of the image, we say the PE has *local support*.

Although neighboring PEs will in general have overlapping regions of support, the design does not restrict the shape of the distributions. Fig. 5 shows a PE where inputs are taken from three separate images, but each image has a different DF. Even though the number

of input samples taken from each image is the same, one support region is relatively "narrow", taking samples that are in close physical proximity, while another region is "broad", taking samples that are sparsely distributed over a larger area.

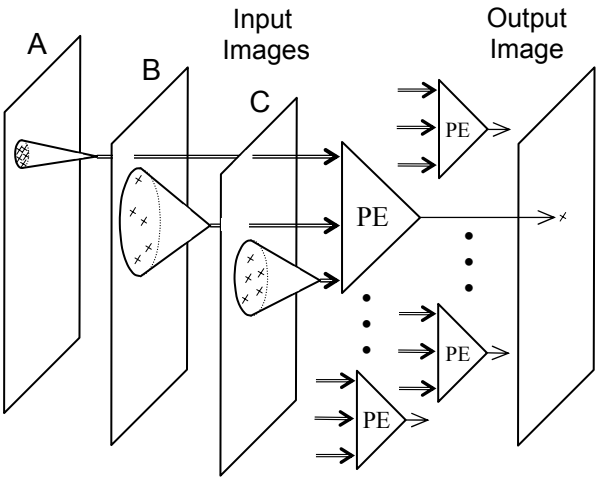

Fig. 5. Processing Elements with local support take their real-valued inputs from small regions in multiple input images and produce a single real-valued output corresponding to a single pixel. The output image is produced by a lattice of PEs operating in parallel. The region of support may be narrow as shown for image *A* or broad as shown for image *B*.

For a direct implementation of a Λ-MAP, the simple design strategy described above and illustrated in Fig. 5 will not work; the output image will consist of a melee of uncoordinated results. The architecture must integrate the results of the individual processing elements into a coherent whole.

2.2. The Ψ-MAP

It is not possible to construct a simple feed-forward implementation of a Λ-MAP using neural networks with local support because there is no way to coordinate the individual PE outputs to form a consistent global image association. It is however possible to construct an SR-MAP. This is because the two Λ-MAPS which make up the SR-MAP form an image loop. The output of any particular PE feeds into the local support of several other PEs in the opposite Λ-MAP. These in turn form many local loops that feed back into the original PE. Figure 6 illustrates how this can occur by showing two connected PEs in the two Λ-MAPs. For illustrative purposes, we show only one PE from each lattice.

In Fig. 6, one PE generates each pixel in the output image. The output of each PE (shown by an "x") together with a few neighboring pixels form the inputs for PEs in the reciprocal Λ-MAP. This process creates numerous interconnected local loops and is the critical step in forming global image association using only local information.

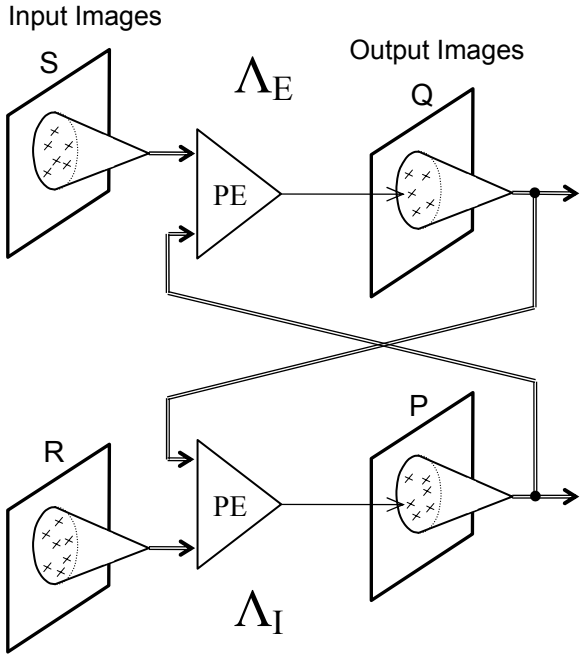

Fig. 6. The Ψ-MAP employs the image feedback loop in the SR-MAP to construct global associations using only local connections. A single recurrence relation between two Processing Elements is illustrated where the output of each PE forms part of the other's input.

Comparing Fig. 6 with the cortical columns shown in Fig. 1, we note several analogies including the local pattern of neuron connections, the extensive number of interconnected loops, and the internal and external laminar structure. Based on these correlations, we use the term Ψ-MAP (Ψ from the Greek word *Psyche*) to refer to a Set-Reset Manifold Association Processor which is constructed from PEs with local support.

3. THE Ψ-MAP ARRAY MODEL

If each Brodmann area corresponds to a unique Ψ-MAP, then the collection of all the Brodmann areas in the cortex constitutes a Ψ-MAP array.

A graphic representation of a Ψ-MAP array is shown in Fig. 7 where the lines denote the transfer of complete images. To simplify the diagram, we use an "I/O Bus" notation where the horizontal rows along the top of the diagram represent the images, and dots are used to illustrate connections. Sensory inputs are transmitted as computational maps as are the motor

control outputs. Each Ψ-MAP generates two output images, corresponding to the two component Λ-MAPs. These are connected figuratively via the I/O bus to other areas. Each Ψ-MAP can have any number of images as inputs, which are integrated together using topographic alignment.

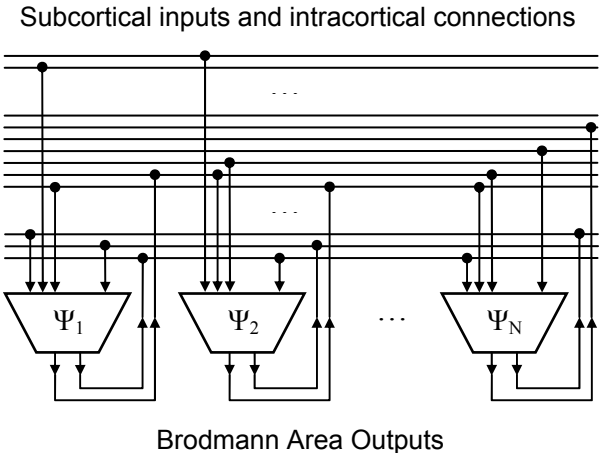

Fig. 7. The Ψ-MAP Array model of the cerebral cortex. Each Ψ-MAP, Ψ_i, corresponds to a separate Brodmann Area. Lines in the diagram correspond to images, and dots represent specific input and output connections.

Each Ψ-MAP in the Ψ-MAP array corresponds to a unique Brodmann area. The number and source of the inputs and the number of associations formed will vary between Ψ-MAPs and even between the internal and external Λ-MAPs of a single Ψ-MAP. These variations will affect the computational requirements of the different cortical layers causing them to vary in thickness between Brodmann areas. However, within a single Brodmann area, the number of associations and the type and origin of the inputs will be the same throughout, suggesting that the thicknesses of the layers should be approximately the same.

Brodmann mapped the cortical regions of many mammals [21] including those of the monkey in diagrams similar to the one shown in Fig. 8. These can be directly correlated with the Ψ-MAP Array model shown in Fig. 7.

An assumption underlying some cognitive models is that during the course of evolution, there was a sudden "break" when the CNS developed a new type of feature extraction mechanism that converted images into tokens, instances taken from a small finite set of discrete symbols. It was then able to manipulate these tokens using a new symbolic processing engine that simultaneously evolved during this same time interval. An alternate hypothesis is that this "break" never took place. Instead, additional general-purpose image association processors, computational engines that had already evolved, were replicated to solve problems of increasing difficulty. Most recently, during the last few million years, the already existing Ψ-MAP array expanded again, adding and integrating new Ψ-MAPs for language and other aspects of abstract reasoning.

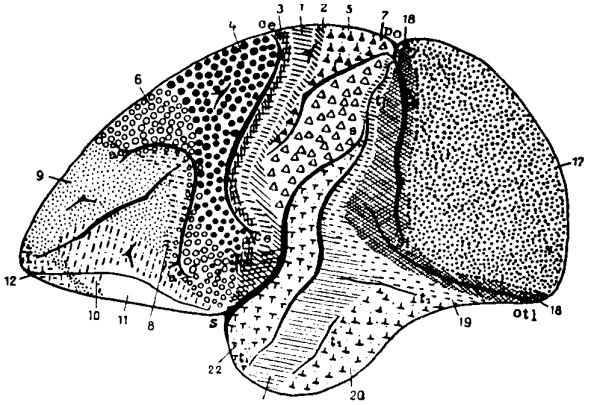

Fig. 8. The Brodmann areas of the monkey cortex. The general principles of operation of a Ψ-MAP Array model can be applied to describe the cerebral cortex of any mammal.

3.1. Attention and Control

Inside every CPU, a control unit coordinates the flow of data between the various components. Every area of the neocortex has reciprocal connections with the thalamus [22], which is known to play an important role in consciousness. Based on observed behavior and the types of real-world problems that the CNS must solve, an agile and flexible control mechanism would be based on image subsets or regions. As a first approximation, we can view these image regions as "control masks" that overlay the Ψ-MAP and regulate the Ψ-MAP processing and Input/Output. The masks blanket the entire extent of the Ψ-MAP "content" images and consequently can be used to identify an arbitrary region within the image. The portions of the MAP images inside the masked region are active while those outside of the region are quiescent.

In this way the thalamus can focus attention on the entire image or on some very small detail. Given the variety of computational maps, control masks can be used to direct our attention to a small region in the visual field, a single sound in a word, a particular part of the body surface, or the motion of a single muscle. Time varying control masks can be used to spatially scan a visual image, or temporally scan through the sounds of a sentence.

3.2. Receptive Fields

Recursion allows neurons with local connections to form global associations. Varying the size of regions from which the neurons make connections, such as those shown in Fig. 5, allows a Ψ-MAP to find the matching image more readily. We can extend this idea by "pre-computing" the average of small image regions with various sizes and using these averages as the inputs to the neurons. Rather than simply using averages, we can further extend this idea by using local spectral functions such as two-dimensional wavelets.

We can associate images by associating their wavelet transforms. The spectral functions used could be identical to the receptive fields in the retina of the eye.

Axons from the *on* and *off-center ganglion cells* in the retina form the optic nerve. These cells receive inputs from nearby photosensitive rods or cones in a roughly circular *receptive field* that contains both a center area and a surrounding ring of opposite polarity. The receptive fields differ in size and are similar to spherically symmetric functions where the variation in the receptive field size is given by *s,* the *scaling* parameter [23]. The axons corresponding to the cells with large and small receptive fields remain segregated as they project to the lateral geniculate nucleus and on to the primary visual cortex (Brodmann area 17) [1], [24]. If we establish a local (*x*, *y*, *z*) coordinate system in the primary visual cortex with the *xy*-plane parallel to the layers of the cortex and the *z*-axis perpendicular to the surface, the size (scale) of the receptive field is topographically mapped to the z dimension. Throughout the cerebral cortex, the layers which make up the cortex have a multi-cellular thickness in the perpendicular *z* direction that gives them a three dimensional structure.

Spectral Ψ-MAPs are based on the following hypothesis: The topographic mapping of receptive fields increasing in size onto the third (*z*) dimension, is not an anomaly unique to visual processing, but rather, a general principle of operation that improves the efficiency and performance of the association computations throughout the entire cerebral cortex.

3.3. Wavelets

In one-dimension, a single main wavelet φ, which is normalized and symmetric about the origin, can generate a family of wavelets at position *x* and scale *s*.

$$\varphi_{x,s}(\xi) = \frac{1}{\sqrt{s}}\varphi\left(\frac{\xi - x}{s}\right) \tag{1}$$

Wavelets with a relatively large value of scaling parameter *s* act as low-frequency wavelets, analogous to broad areas of support, and those with a relatively small value of *s* act as high-frequency wavelets, analogous to narrow regions of support.

The wavelet transform of a function *f* is given by

$$\begin{aligned}\mathcal{W}[f](x,s) &= \int_{-\infty}^{+\infty} f(\xi)\varphi^*_{x,s}(\xi)\,d\xi \\ &= \left\langle f, \varphi_{x,s}\right\rangle\end{aligned} \tag{2}$$

where φ^* denotes the complex conjugate of φ.

Several methods are available for generating sets of multidimensional wavelets whose linear combinations are dense in $\mathbf{L}^2(\mathbb{R}^n)$. Of particular interest are spherically symmetric wavelets, which can be expressed in the form $\varphi(\mathbf{x}) = f(\|\mathbf{x}\|);\ \mathbf{x} \in \mathbb{R}^n$ for some one-dimensional function *f*. The scale parameter for spherically symmetric wavelets is a single real-valued positive number $s \in \mathbb{R}_+$. Therefore, the overall parameter space has dimension *n*+1. While some wavelets, such as the normalized second derivative of a Gaussian function, have non-zero values out to infinity, we are mainly interested in wavelets with compact support [25], in particular wavelets that are zero outside a small local region.

If a wavelet is spherically symmetric, so is its Fourier transform. Thus, $\hat{\varphi}(\boldsymbol{\omega}) = \chi(\|\boldsymbol{\omega}\|)$ for some function χ, and the admissibility condition [7] is

$$C_\chi = \int_0^{+\infty} \frac{|\chi(\omega)|^2}{\omega}\,d\omega < \infty. \tag{3}$$

For $f \in \mathbf{L}^2(\mathbb{R}^n)$ the wavelet transform, $\tilde{f}$, is defined by extending the integral in (2) to *n* dimensions. The inverse wavelet transform in *n* dimensions [25] [26] is given by

$$\begin{aligned}f(\boldsymbol{\xi}) &= \mathcal{W}^{-1}[\tilde{f}](\boldsymbol{\xi}) \\ &= \frac{1}{C_\chi}\int_{\mathbb{R}_+}\int_{\mathbb{R}^n} \tilde{f}(\mathbf{x},s)\varphi_{\mathbf{x},s}(\boldsymbol{\xi})\,d\mathbf{x}\,\frac{ds}{s^{n+1}}.\end{aligned} \tag{4}$$

Wavelet transforms on spherical surfaces are widely used in science and can be defined on other manifolds as well using the inner product [25].

3.4. Spectral Ψ-MAPs

Each of the Brodmann areas $\{\Psi_i\}$ has a unique shape that projects along the perpendicular direction of the cortical columns onto a two-dimensional manifold $\mathbb{M}_i$. The spectral functions within each cortical layer are parameterized by a center position (*x*,*y*) and a single real-valued scale factor $s \in \mathbb{R}_+$. The

resulting three-dimensional manifold $\mathbb{J}_i = (\mathbb{M}_i \times \mathbb{R}_+)$, maps to a single cortical layer of a single Brodmann area.

Examining the Ψ-MAP shown in Fig. 6, we now replace the two-dimensional images with three-dimensional "slabs" of thickness z_0. The scaling parameter $s \in (0,\infty)$ is monotonically mapped to the interval $(0, z_0)$ that corresponds to the physical thickness of a single cortical layer in a particular Brodmann area. In the resulting three-dimensional spectral manifold, the pixels shown in Fig. 6 now correspond to voxels that represent the magnitude coefficients of specific spectral functions. A processing element PE takes as inputs, voxels in a three-dimensional spectral manifold, and produces as a result, a single voxel in a three-dimensional output spectral manifold.

Low-frequency spectral functions measure components over a large area of an image. Consequently, even though the PE has only local connections near an image point (x_0, y_0), if the connections extend through the entire thickness of the cortical layer, its output value can change based on changes in the input image from the finest to the coarsest levels of detail. Moreover, the recursion in the Ψ-MAP allows the output values of PEs that correspond to low-frequency spectral functions to propagate quickly throughout the entire MAP.

3.5. Orthogonal Projections

Because of the scale parameter *s*, the spectral manifold on which $\mathcal{W}[f](x,y,s)$ is defined is three-dimensional. Since this spectral manifold has a higher dimension than the original two-dimensional image space, there are many spectral functions for which there is no corresponding image. Mathematically, almost all functions *h*, defined on the space of continuous wavelet transforms, do not have a well-defined inverse $\mathcal{W}^{-1}[h]$.

Consequently, the space of transformed functions is over-specified and contains redundant information. This redundancy can be used to reduce errors and create "energy minimums" where the Ψ-MAP images lock each other in place.

The PEs compute the required outputs for a large number of stored associations based on only limited local information. Consequently, the overall result of these calculations can only be an approximation, which may not have a well-defined inverse. However, using the *reproducing kernel* it is possible to estimate the approximation error and calculate the closest function for which the inverse spectral transformation exists.

For the one-dimensional case, the following equation defines the necessary and sufficient conditions for a function $\mathcal{W}[f]$ to be a wavelet transform [7].

$$\mathcal{W}[f](x,s) = \frac{1}{C_\varphi}\int_0^{+\infty}\int_{-\infty}^{+\infty}\mathcal{W}[f](\xi,\eta)K(x,s,\xi,\eta)\,d\xi\,\frac{d\eta}{\eta^2} \quad (5)$$

where the constant C_φ is given by (3). The reproducing kernel *K* measures the correlation between the wavelets $\varphi_{x,s}(\alpha)$ and $\varphi_{\xi,\eta}(\alpha)$ and is defined by

$$\begin{aligned} K(x,s,\xi,\eta) &= \int_{-\infty}^{+\infty}\varphi_{x,s}(\alpha)\,\varphi_{\xi,\eta}(\alpha)\,d\alpha \\ &= \left\langle \varphi_{x,s}, \varphi_{\xi,\eta} \right\rangle. \end{aligned} \quad (6)$$

Let $H = \mathbf{L}^2(\mathbb{R}\times\mathbb{R}_+)$ and let *U* denote the linear subspace of *H* where the inverse wavelet transform exists. Using the reproducing kernel specified by (6) we define the linear operator $\mathcal{V}$ by

$$\mathcal{V}[f](x,s) = \frac{1}{C_\varphi}\int_0^{+\infty}\int_{-\infty}^{+\infty} f(\xi,\eta)K(x,s,\xi,\eta)\,d\xi\,\frac{d\eta}{\eta^2} \quad (7)$$

From (5) we note that for $f \in U$, $\mathcal{V}[f] = f$. In a straightforward proof, it can be shown that $\mathcal{V}$ is an orthogonal projection of *H* onto *U*. If we view the local estimation errors in the calculations as additive noise $e(x,s)$, then

$$\mathcal{V}[f+e] = f + \mathcal{V}[e] \quad (8)$$

Since $\mathcal{V}$ is an orthogonal projection, $\|\mathcal{V}[e]\| \le \|e\|$. That is, $\mathcal{V}$ removes the component of the noise that is in $U^\perp$ and thereby projects the estimate to a function that is closer to the correct solution *f*.

This orthogonal projection can be used to create stability in the Ψ-MAP associations by forming "basins" around valid wavelet transforms where small errors result in invalid spectra, which are subsequently removed or greatly reduced by (7). When used in conjunction with a pattern recognition model based on neurotransmitter fields [27] this projection can extend the region of stability.

From the definition of the reproducing kernel (6), we can see that at a fixed position (x_0, s_0) in the spectral manifold, the kernel $K(x_0, s_0, \xi, \eta)$ is zero for values of (ξ,η) where the spectral functions φ_{x_0,s_0} and $\varphi_{\xi,\eta}$ do not overlap. Moreover, *K* is defined in terms of the wavelets themselves and does not depend on the transformed function *f*. Consequently, the kernel *K* can be pre-computed (and encoded in synaptic weights). The projection defined by (7) can then be evaluated dynamically at each point (*x*, *s*).

We have discussed the reproducing kernel only for the case of one-dimensional wavelets $\varphi_{x,s}$. However, the definition (6) is expressed in terms of an inner product, and in general, reproducing kernels only require the mathematical structure of a Hilbert space [28][29].

4. A Ψ-MAP IMPLEMENTATION

It is possible to design several types of Ψ-MAPs using local processing elements. Fig. 9 shows a detailed Ψ-MAP design that illustrates one possible architecture. Variations of this design can achieve the same or similar functionality.

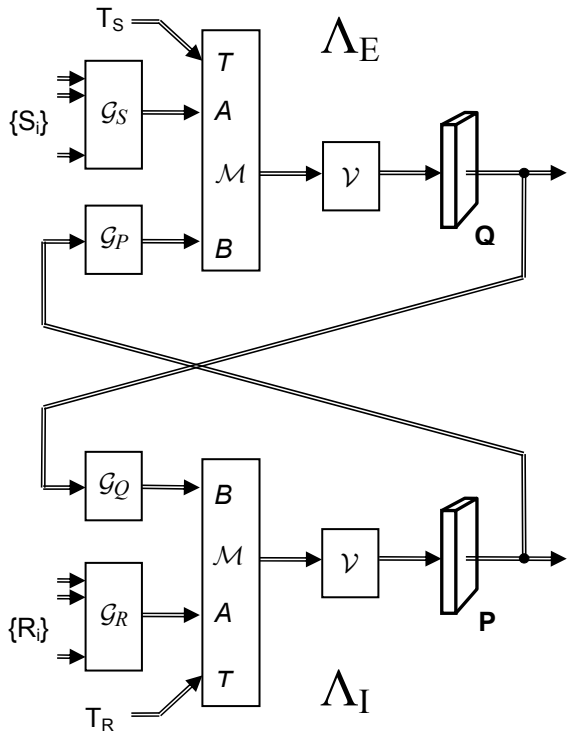

Fig. 9. A detailed Ψ-MAP implementation illustrates the general pattern of interconnection. $\mathcal{G}$ denotes a neural network association operation, $\mathcal{M}$ denotes the masking and multiplexing operation and $\mathcal{V}$ denotes the orthogonal projection based on the reproducing kernel.

The double lines in Fig. 4 represent the transfer of data defined on three-dimensional spectral manifolds. The letter $\mathcal{G}$ denotes a general association neural network such as the lattice of processors shown in Fig. 5, the letter $\mathcal{V}$ denotes orthogonal projections based on the reproducing kernel, and the vertical box marked $\mathcal{M}$ performs multiplexing operations based upon the mask inputs marked T_S and T_R. Each box labeled $\mathcal{G}$ is trained with a different set of input and output relationships and consequently carries a subscript that identifies it as a unique transform.

The inputs, $\{s_k\}$ and $\{r_k\}$, represent collections of image spectra that arise from either subcortical regions or from the outputs of other Brodmann areas. The integration of data from three separate input images to form a single output pixel was illustrated in Fig. 5. If $\mathcal{G}_S$ (or $\mathcal{G}_R$) forms the same output association for several members of a given collection of inputs $\{s_i\}$ (or $\{r_i\}$), then the associations will mutually reinforce one another. Consequently, even though single inputs may not be sufficiently strong to bring forth a recollection, multiple inputs will add "context", and their combined effect may surpass a threshold required to evoke the entire memory.

The multiplexor masks allow the system to focus attention on selected regions and to control whether individual Brodmann areas accept new inputs or retain their current contents. Each of the reciprocal Λ-MAPs, shown in Fig. 9, contains two separate, association networks whose outputs feed into the *A* and *B* inputs of the multiplexor box labeled $\mathcal{M}$. A third input, labeled *T*, shown with a diagonal line, is the control mask.

Let $\alpha(x, y, s)$ be one of the mask signals T_S or T_R. These can control the multiplexor by performing an operation analogous to the *alpha blending* calculation, $(1-\alpha)A + \alpha B$, used for image composition in computer graphics [30]. For voxels where $\alpha = 0$, the output equals *A*, and where $\alpha = 1$, the output equals *B*. Values in between smoothly blend the two images.

When the spectral coefficients are not based on a set of orthogonal functions, the result of an association formed by a real-valued neural network will usually contain small errors that result in invalid spectral representations. Moreover, the masking operation may also result in a spectral function that does not correspond to the transform of an actual image. However, using the reproducing kernel (6) we can project these functions using the linear operator $\mathcal{V}$ given by (7) to the nearest function for which the inverse transform $\mathcal{W}^{-1}$ produces a valid result. This operation is shown in Fig. 9 following the multiplexing operation. Since the results of the orthogonal projections are *Q* and *P*, we thereby guarantee that the spectral outputs of a Ψ-MAP always correspond to valid images.

As long as the control signal $\alpha(x, y, s)$ is identically equal to one, in both the exterior and interior Λ-MAPs, the Ψ-MAP will ignore its inputs and retain its current stored value. Under these conditions, the Ψ-MAP is *latched* and the contents of this short-term memory remain fixed on the outputs *q* and *p*.

5. CONCLUSIONS

The description presented in this paper is primarily concerned with static structure, but provides a basis for the dynamic models that are necessary to characterize cognitive functions such as language production and understanding. Additional work will be required to analyze the many trade-offs involving various spectral functions, masking algorithms, and Ψ-MAP architectures. Neural models, in particular those defined by neurotransmitter field theory, directly affect how the processing elements learn and recall associations.

The Ψ-MAP is a new type of image centric processing architecture, which combines several design elements including recurrent neural networks, locally connected processing elements, image masks, spectral transformations, and an orthogonal projection based on the reproducing kernel. The Ψ-MAP Array model has many correlations with the neurological organization of the cerebral cortex and may help provide insight into the nature of memory and cognition.

Acknowledgements

The author would like to thank Professor M. Tuceryan for his encouragement and helpful comments. This document contains material that is patent pending by General Manifolds LLC, http://www.gmanif.com/ip.

References

[1] E. R. Kandel, J. H. Schwartz, & T. M. Jessell, *Principles of neural science* (4th ed.), New York: McGraw-Hill, 2000.

[2] B. Garoutte, *Survey of Functional Neuroanatomy* (3rd ed.), California: Mill Valley Medical, 1994.

[3] M. Spivak, *A comprehensive introduction to differential geometry* (3rd ed.), Wilmington, DE: Publish or Perish, 1979.

[4] B. Schutz, *Geometric methods of mathematical physics*, Cambridge: Cambridge University Press, 1980.

[5] E. I. Knudsen, S. du Lac, & S. D. Esterly, "Computational maps in the brain," *Ann. Rev. of Neuroscience*, vol. 10, pp. 41-65, 1987.

[6] D. S. Greer, "A unified system of computational manifolds," *Tech. Rep. TR-CIS-0602-03*, Dept. of Comp. and Info. Sci., IUPUI, Indianapolis, IN, 2003.

[7] S. Mallat, *A Wavelet Tour of Signal Processing* (2nd ed.), San Diego: Academic Press, 1999.

[8] Y. Wang, "The cognitve processes of abstraction and formal inferences," *Proc. 4th IEEE International Conf. on Cognitive Informatics (ICCI'05)*, Irvine, California, 2005.

[9] Y. Wang, "The theoretical framework of cognitve informatics," *International J. of Cognitve Informaics and Natural Intelligence*, 1(1), pp. 1-27, 2007.

[10] Y.Y. Yao, "Concept formation and learning: a cognitive infomatics perspective," *Proc. 3rd IEEE International Conf. on Cognitive Informatics (ICCI'04)*, Victoria, Canada, 2004.

[11] V. Prince, & M. Lafourcade, "Mixing semantic networks and conceptual vectors application to hyperonymy," *IEEE Trans. Systems, Man and Cybernetics, C*, vol. 36. pp. 152-160, 2006.

[12] D. J. Willshaw, O. P. Buneman, & H. C. Longuet-Higgins, "Non-holographic associative memory," *Nature,* Vol. 222, pp. 960-962, 1969.

[13] Kosko, B. (1988). "Bidirectional associative memories," *IEEE Trans. Systems, Man and Cybernetics,* vol. 18, pp. 49-60, Jan. 1988.

[14] Z. Xu, Y. Leung, & X. He, "Asymmetrical bidirectional associative memories," *IEEE Trans. Systems, Man, and Cybernetics*, vol. 24, pp. 1558-1564, Oct. 1994.

[15] L. O. Chua, & L. Yang, "Cellular neural networks: theory," *IEEE Trans. Circuits and Systems*, vol. 35(10), pp. 1257-1272, 1988.

[16] Q. Zhang, & A. Benveniste, "Wavelet Networks," *IEEE Trans. Neural Networks*, vol. 3 (6), pp. 889-898, 1992.

[17] M. Thuillard, "A review of wavelet networks, wavenets, fuzzy wavenets and their applications," in *Advances in Computational Intelligence and Learning: Methods and Appl*. Deventer: Kluwer, 2002.

[18] S. S. Iyengar, E. C. Cho, & V. V. Phoha, *Foundations of Wavelet Networks and Applications*, Boca Raton: Chapman & Hall / CRC, 2002.

[19] D. S. Greer, "A model of natural computation based on recurrent neural networks and reciprocal images," *Conf. on Computational Intelligence*, IASTED 2006.

[20] B. V. Gnedenko, *The Theory of Probability*. (Seckler, B. D. Trans.) New York: Chelsea, 1968.

[21] C. B. von Economo, & G. N. Koskinas, *The Cytoarchitectonics of the Adult Human Cortex*, (trans. H. L. Seldon), Springer Verlag 1925.

[22] T. E. J. Behrens, H. Johansen-Berg, M. W. Woolrich, S. M. Smith, C. A. M. Wheeler-Kingshott, P. A. Boulby, et al. "Non-invasive mapping of connections between human thalamus and cortex using diffusion imaging," *Nature Neuroscience,* vol. 6 (7), pp. 750-757, 2003.

[23] R. Nevatia, *Machine Perception*, Englewood Cliffs: Prentice-Hall, 1982.

[24] P. Churchland, & T. J. Sejnowski, *The Computational Brain*, Cambridge: MIT Press, 1994.

[25] I. Daubechies, *Ten Lectures on Wavelets*, Philadelphia, Society for Industrial and Applied Mathematics, 1992.

[26] P. S. Addison, *The Illustrated Wavelet Transform Handbook*, Bristol, UK: Institute of Physics Publishing, 2002.

[27] D. S. Greer, "Neurotransmitter fields," *Proc. of International Conf. on Artificial Neural Networks*, (ICANN'07), Porto, Portugal, 2007 (in press).

[28] N. Aronszajn, "Theory of reproducing kernels," *Trans. of the American Mathemtacial Society*, vol. 68 (3), pp. 337-404, 1950.

[29] S. Saitoh, *Integral Transforms, Reproducing Kernels and their Applications*. Essex: Addison Wesley Longman, 1997.

[30] K. Thompson, "Alpha blending," In A. Glassner (Eds.), *Graphics Gems*, pp 210-211, Cambridge: Academic Press, 1990.